Effects of Carbon Fiber Reinforced Plastic Laminate on the Strength of Adhesive Joints

N. A. Yahya
Zawia University, Faculty of Engineering, Department of
Mechanical and Industrial Engineering, Zawia, Libya.
nyahya@zu.edu.ly

Abstract— **Carbon fiber composites are being widely considered for many classes of heavily loaded components. A common feature of such components is the need to introduce local or global loads into the composite structure. The use of adhesive bonding rather than mechanical fasteners offers the potential for reduced weight and cost. The use of carbon fiber reinforced plastics (CFRP) for the repair of steel structure is also advantageous, for example to avoid welding or bolting which can weaken structure and add fire risk. This study is based on adhesive bonded double lap shear (DLS) joints where the inner adherend is steel and the outer adherend is cross plies unidirectional (UD) CFRP. Overlap lengths of 25-125 mm with CFRP thickness of 3 and 6 mm were considered and two different orientation angles [0^o,90^o] and [90^o,0^o] laminates have been considered. The overall objectives of the paper are to investigate the delamination of the CFRP laminates within the DLS joints under quasi-static loading and both experimental and numerical techniques were used. The numerical study was based on 2-D model using strength-limit method, taking into consideration the UD properties of the plies and the resin layers separating these. As a result, it was concluded that the data obtained from 2-D finite element analysis were coherent with experimental results and additional to that fiber orientation angles of the laminate markedly affected the failure load of joints, failure mode and stress distributions appeared in adhesive and composite.**

Index Terms: **Adhesive joints, Composites, Delamination, Finite element stress analysis.**

I. INTRODUCTION

Adhesive bonding applications are used widely in industry because of the advantages such as uniform stress distribution, the ability to join different materials and design flexibility. Adhesive bonding provides several advantages over riveting and bolting, such as reduction of stress concentrations, reduced weight penalty and easy manufacturing [1]. The use of CFRP for the repair of steel structure is also advantageous, for example to avoid welding or bolting which can weaken structure and add fire risk. Any successful applications of steel/composite connections, however, require understanding the structural behaviour and failure of these connections.

Received 24 Sept 2017; revised 25 October 2017; accepted 27 October 2017.

Available online 30 October 2017.

This study is based on adhesive bonded DLS joints where the inner adherend is steel and the outer adherend is unidirectional CFRP. Different approaches were employed in the past to predict the mechanical behaviour of bonded assemblies. In the FEA work on bonded assemblies research dates back to the 1970s when Wooley and Carver [2] conducted a stress analysis on single lap joint. On the strength prediction of bonded assemblies, the strength of materials approach is based on the evaluation of allowable stresses [3, 4] or strains [5] by theoretical formulations or the FEA. The assembly strength can be predicted by comparing the respective equivalent stresses or strains at critical regions obtained by stress or strain-based criteria, with the properties of the structure. These criteria are highly mesh dependent, as stress singularities are present at the end of the overlap regions especially at sharp corners [6]. Numerical methods provide a general tool for analysis of arbitrary geometries and loading conditions. Among the numerical methods, finite element method (FEM) has been extensively used with success and countless studies on various adhesively bonded joints via this technique were performed by many authors [7-10]. The use of FEM to study adhesively bonded joints with composite adherends has brought a new level of understanding of these structures [11].

One approach to ensuring reliability in bonded joints between metallic adherends is to ensure that the overlap length is substantially higher than that required to carry the load across the joint. This has the effect of greatly de-stressing the mid-section of the joint [12], and to a very large extent, ensures that cracking initiates at the end of the joint and may propagate along the joint for some substantial distance before reaching criticality [13]. For high toughness, adhesive systems, the propagation rate can be sufficiently low that critical structures may be safely assigned an inspection and maintenance schedule. For composite materials, the situation is somewhat different. This is due to the anisotropy inherent in laminated composites. Even for a quasi-isotropic laminate, the in-plane and through-thickness strengths are very different. With poorly designed joints between composites, the initial failure may be by through thickness tensile failure of the laminate rather than by crack initiation in the adhesive [14]. The interlaminar fracture toughness of most carbon fiber laminates is substantially lower than that of typical structural adhesives. It is also very sensitive to material quality and can be sensitive to the operating environment [15].

The work in this paper is presents an experimental and numerical study of the tensile behaviour of two-dimensional steel/CFRP laminate connections, using the commercial software ABAQUS. The objectives of the simulations are to obtain stress distributions and to evaluate the failure load of the joint to assess the effect of geometric changes in the CFRP laminates on the joint strength. The results of these simulations have been used to describe and confirm the experimental observations.

II. EXPERIMENTAL WORK

A. Geometry and Dimensions of DLS joints

The DLS joint geometry and dimensions are represented in Figure 1. The joint was made up of two mild steel inner adherends and two outer adherends made from the CFRP materials. The width of all specimens was 25 mm, adhesive thickness, t_a= 0.2 mm and the thickness of inner adherends is 10 mm. The overall length remained constant i.e. 430 mm varies overlaps were used. Two different values of outer adherend thickness, namely 3 mm and 6 mm for 12 layers and 24 layers respectively, and five values of overlap length OL (25, 50, 75, 100 and 125 mm) were evaluated, see Figure 2.

The bonding surfaces for steel substrates were prepared by grit blasting to improve the effectiveness of the adhesive bond [16]. The final stage of the process is to clean any contaminants that have formed on the steel substrates after the grit blasting; this was done by cleaning the surface with the use of an acetone solution. Light grade P120C silicon carbide paper was used for outer adherents (CFRP laminate) to clean the bond area and eliminate unevenness in the bonding surfaces. This was followed by acetone cleaning, drying and adhesive application. After the assembly, the specimens were cured in an oven under a uniform pressure loading. According to adhesive material manufacturer curing procedure consisted of heating the specimens in 80^{o}C for one hour, followed by a slow cooling to ambient temperature.

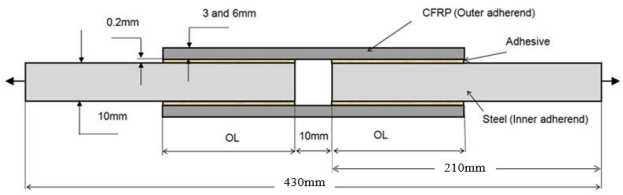

Figure 1. DLS Joint Geometry and Dimensions.

Also, various ply orientations for the composite were used, including [0^o,90^o] and [90^o,0^o]. For example, the first ply of the [0^o,90^o] lay-up had the UD fibers orientated at 0^o relative to the direction of the applied load. The type and details of the specimens used for tensile testing are presented in Table 1. The designations for the CFRP adherend are used to describe the types of the specimens. This also indicates the orientation of the UD fiber and total laminate thickness.

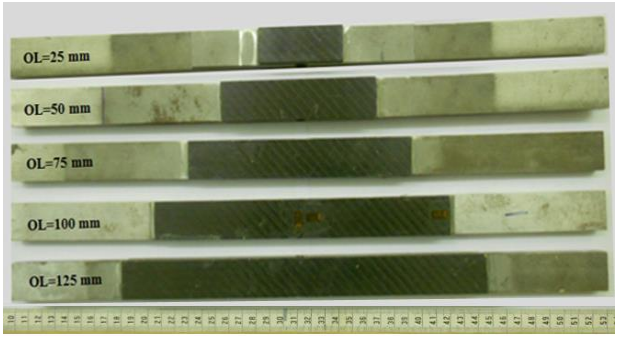

Figure 2. Bonded Specimens Showing [0^o,90^o]$_6$ Specimens with Various Overlap Lengths.

Table 1: Type and Number of Specimens

Specimen type	Overlap length (mm)	CFRP adherend thickness (mm)	Number of specimens
[0^o,90^o]$_6$	25	3	5
	50	3	6
	75	3	6
	100	3	5*
	125	3	4**
[90^o,0^o]$_6$	25	3	6
	50	3	6
	75	3	6
	100	3	4*
	125	3	3**
[90^o,0^o]$_{12}$	25	6	4*
	50	6	3**

* One of these was discarded due to bonding defects.
** Limited number due to materials availability.

B. Tensile Testing Set-up

The setup for the experiments can be seen in Fig 3. The testing used a Zwick/Roell 250 kN Universal testing machine which provided load and extension data for each test. Each specimen was gripped at 50 mm from the edge at both ends. The loading rate was 0.5 mm/min, and all tests were performed at room temperature.

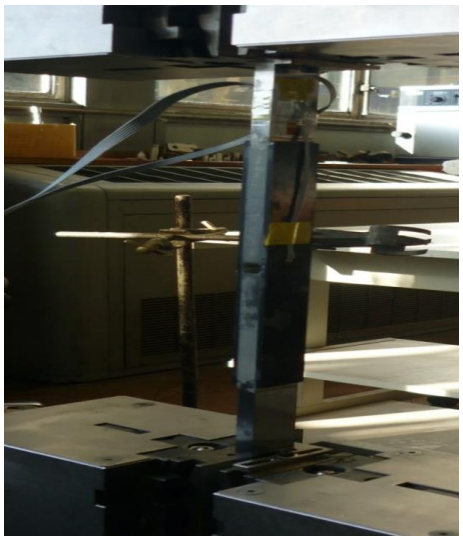

Figure 3. Tensile Test of [0^o,90^o]$_6$ Specimen with 75 mm Overlap Length.

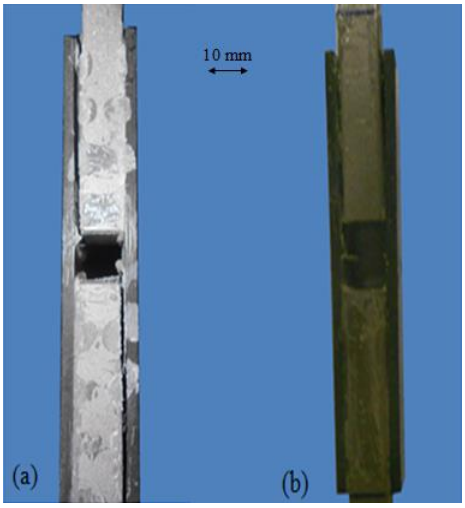

Figure 4. Failure Shapes: a) S-shape, b) U-Shape.

The load and displacement values were recorded to give the failure load. The specimens were clamped at either end and then pulled apart until failure. This process was completed for all different joints. The reasoning for this was to find the effects of increasing the joint overlap, changing the laminate direction and outer adherend thickness on the type of fracture, and the peak load of the joint. During the testing of DLS joints, the failure path of the specimens occurred in the form of an S-shape or U-shape, as shown in Figure 4a and b.

C. Test Results

One of the most important parameters that influence the joint strength is the overlap length. Tests were conducted to determine the effects of this on the strength of the joint. Overlap lengths of 25–125 mm was considered for the $[0^o,90^o]_6$ and $[90^o,0^o]_6$ specimen. The test results for these are shown in Figure 5. For shorter overlaps (25–50 mm), failure load seems to be proportional to overlap length. For longer overlaps (75–125 mm), failure load tends to reach a plateau independent of the overlap length. Similar experimental results were observed in other work [17]. Also, the effect of fiber direction was considered for specimens. Figure 5 shows the mean values of the maximum failure loads for the two fabric orientations. The results show that the $[0^o,90^o]_6$ specimen produced 5% higher strength than the $[90^o,0^o]_6$ specimen. The reason for the small difference for the $[0^o,90^o]_6$ and $[90^o,0^o]_6$ specimens are their equal global axial stiffness and strength. The effect of laminate thickness was considered for specimens. The failure load prediction by experimental for the $[90^o,0^o]_6$ and $[90^o,0^o]_{12}$ specimens with varying adherend thicknesses are shown in Figure 6, this shows the effect of increasing adherend thickness and indicate an increase of joint strength with an increase in laminate thickness. For example, there is an 10% increase in joint strength as a result of increasing the thickness from 3 mm to 6 mm. Figure 7 shows the failure surfaces of these joints. For the $[0^o,90^o]_6$ specimen, failure is apparently in the adhesive (adhesion failure). It may be noticed from Figure 7(a) that the adhesive residues are left on both the steel and composite adherends. For the $[90^o,0^o]_6$ specimen, the failure can be characterised as delamination in the composite (adherend failure) as shown in Figure 7(b). Failure in this case is likely to have started within the resin due to in-plane transverse stress and/or interlaminar failure between the top two plies.

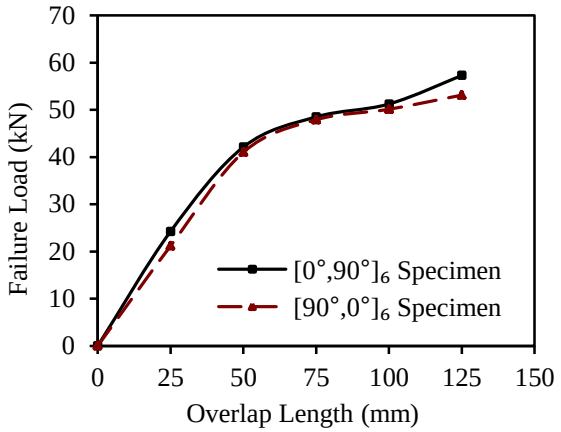

Figure 5. Overlap Length Effect on the Failure Load for $[0^o,90^o]_6$ and $[90^o,0^o]_6$ Lamina.

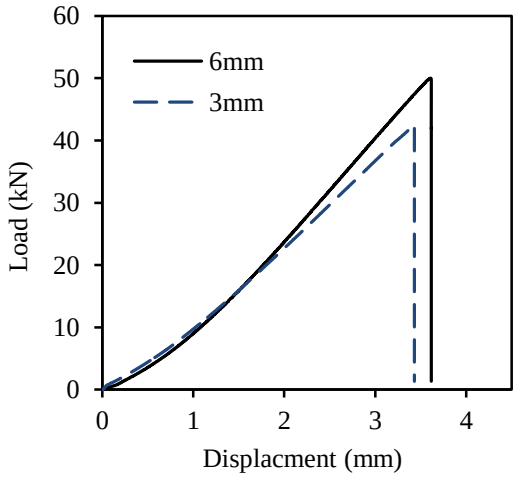

Figure 6. Load-Displacement Relations for Different Laminate Thickness for $[90^o,0^o]_6$ and $[90^o,0^o]_{12}$ Lamina with 50 mm Overlap Length.

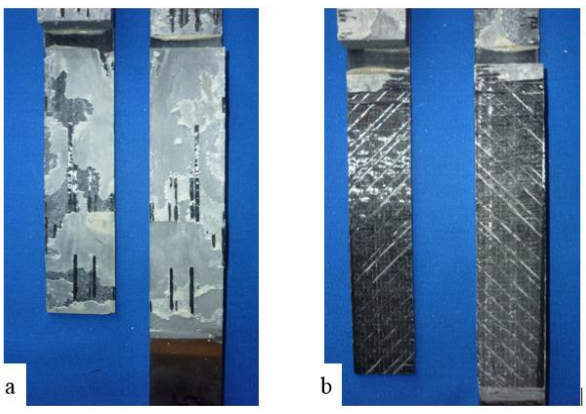

Figure 7. Experimental Fracture Surfaces for DLS joint: (a) with $[0^o,90^o]_6$ Laminate and (b) with $[90^o,0^o]_6$ Laminate.

III. NUMERICAL ANALYSIS

A commercially available finite element code, ABAQUS, was used for the numerical analysis. The geometry and meshing of the two-dimensional (2D) model was carried out using Abaqus/CAE. The geometry of DLS joint is symmetry, the joint can be simplified to one quarter of the specimen, thus made the model very easier to create and reduce the complexity of the FEA simulation and reduce computation time. 2D model was used taking into consideration the non-linear material and geometry factors, using the plain-strain quadratic elements and rectangular eight-node finite elements, CPE8R (reduced integration). Figure 8 illustrates the boundary conditions. The mechanical properties of various materials for the joints are presented in Table 2. The Young's modulus and the shear modulus of the bulk adhesive [17] and rich resin [18, 19] .In this analysis an attempt was made to model the CFRP laminate in its constituent parts of resin and unidirectional laminates. Each ply was modelled to refeect the 90° and 0° directions. The epoxy resin was modelled with its isotropic elastic properties. The adhesives were asigned elasto-plastic properties. The stress magnitude will be subsequently evaluated at 0.025 mm away from free surface , also with the node at the free edge being ignored due to spurious effects at this point as a result of the stress tip singularity [20, 21].In this work the maximum shear and peel stresses for the adhesive are considered as failure criteria. Also some critical stresses within the CFRP were considered, including interlaminar tensile stresses and longitudinal stresses.

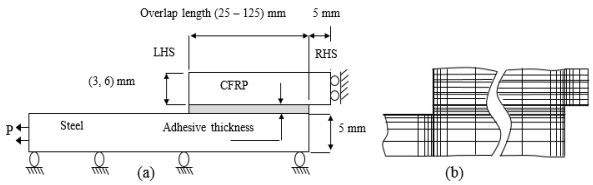

Figure 8. (a) Boundary and LOading Conditions; and (b) Finite Element Mesh of the DLS Joint

Table 2. Material Properties of Carbon-epoxy Composite, Adhesive and Mild Steel.

Property		Carbon fiber lamina	Epoxy adhesive Araldite 2015	Epoxy resin LY3505/ XB3405	Mild Steel
Young's Modulus (GPa)	E_{11}	139.4	1.8	3.5	210
	E_{22}	7.66	-	-	-
	E_{33}	7.66	-	-	-
Shear Modulus (GPa)	G_{12}	3.68	0.662	1.296	-
	G_{13}	3.68	-	-	-
	G_{23}	2.94	-	-	-
Poisson's ratio	ν_{12}	0.26	0.36	0.35	0.3
	ν_{13}	0.26	-	-	-
	ν_{23}	0.304	-	-	-
Tensile strength (MPa)		1400	40	85	450
Transverse strength (MPa)		86	-	-	-

IV. RESULTS AND DISCUSSION

A. *Failure Prediction*

The strength-limit modelling seems to give a reasonable correlation with maximum stress values of the materials at failure load. The degree of correlation depends of the geometry of the joints in terms of CFRP thickness and length of overlap. Among the failure criteria that have been employed are tensile stress of the adhesive and resin at the RHS of the joint, which may have referred to as peel stress. Also, the longitudinal tensile strength of the CFRP may be used especially in the case of thin outer adherend. Another important measure of joint failure is the level of the plastic shear stress within a joint.

B. *Effect of Overlap Length*

Figure 9 showed the shear stress along the adhesive/composite interface for all joints [0°,90°] with different overlap lengths being high at the RHS near the centre of the joint. The length of plastic zone for the 25 mm and 50 mm overlap joints is about 50% of the overlap.

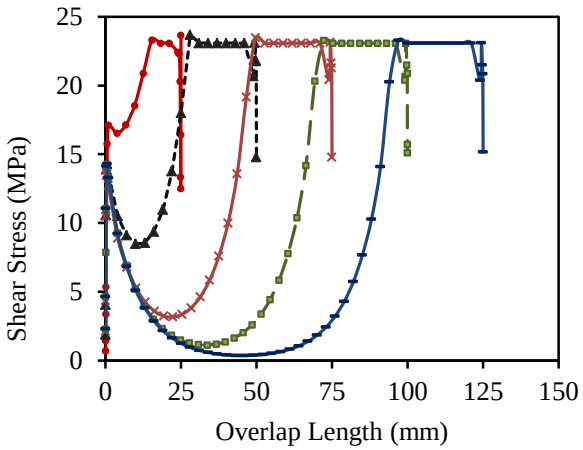

Figure 9. Shear Stress Distributions Along the Upper of Adhesive Layer for Different Values of Overlap Length for $[0^o,90^o]_6$ Models at Failure Loads.

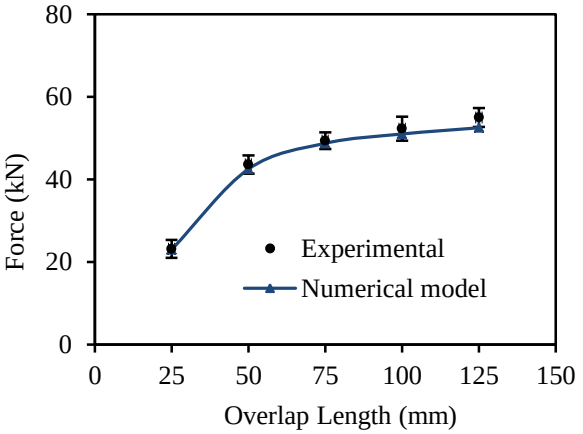

Figure 10. Experimental Failure Loads vs. Numerical Prediction for Different Overlap Length

For overlaps greater or equal to 75 mm the maximum stress remained almost constant, and the plastic zone

length being about 30 mm. This has a good practical dimension as structural joints in marine construction, for example, are expected to be in excess of a 100 mm overlap. Figure 10 shows a comparison between the experimental failure loads and the prediction for the numerical method.

C. *Effect of Adherend Thickness*

Figure 11 illustrates the shear and peel stress results from both the end of the joint overlap (LHS) and at the joint centre (RHS) for two models. The models are based on $[90^o,0^o]_6$ and $[90^o,0^o]_{12}$ UD laminates with two thickness values of 3 mm and 6 mm (all 50 mm overlap). Loading of each model was 43 kN applied at the steel adherend as a tensile load. The shear stress and peel stress occur in the same position for every joint. This position is 0.025 mm from the inner adherend edge at the joint centre (RHS). The peak values at the end of the joint overlap also occur at the same position, 0.3 mm from the upper adherend edge (LHS).

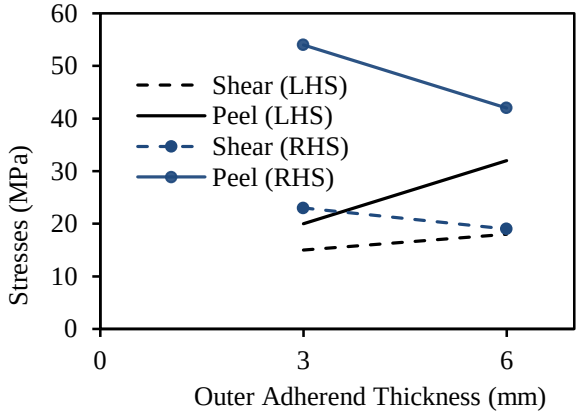

Figure 11. Influence of the Laminate Thickness on the Peel and Shear Stresses. (See Figure 8a).

According to the results it is clear the main area of concern is towards the centre of the joint. The effect of increased laminate thickness shows significant reductions in the stress levels occurring at the joint centre, especially in the peel stress Figure 11.

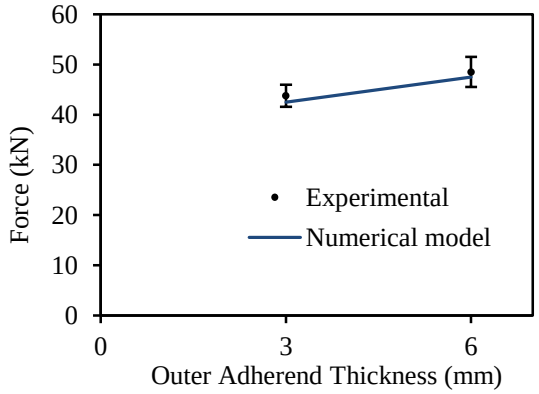

Figure 12. The Effect of the Laminate Thickness on the Failure Load.

In addition, the failure load prediction by both experimental and numerical techniques were used showed that increasing the CFRP laminate thickness leads to an increase the failure loads (Figure 12).

D. *Effect of Stacking Sequence*

The models $[0^o,90^o]_6$ and $[90^o,0^o]_6$with 75 mm overlap were used to study the effect of orientations on stress distribution in each model. The mechanisms of failure of these models with different orientations are presented in Figure 13, which shows the contours of maximum principal stresses for these joints. The maximum stresses occur at the center of the joint (RHS - Figure 8). The maximum principal stress distribution along the upper interface of the adhesive layer is shown in Figure 14 with the peak stresses for the both cases at the RHS of the joint.

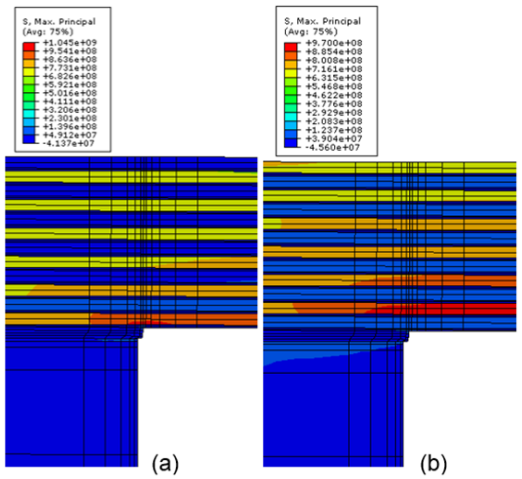

Figure 13. Contours of Maximum Principal Stress in the CFRP for Different Models with 75 mm Overlap: (a) $[0^o,90^o]_6$ and (b) $[90^o,0^o]_6$ at Failure Loads (50 kN and 47.5 kN) Respectively.

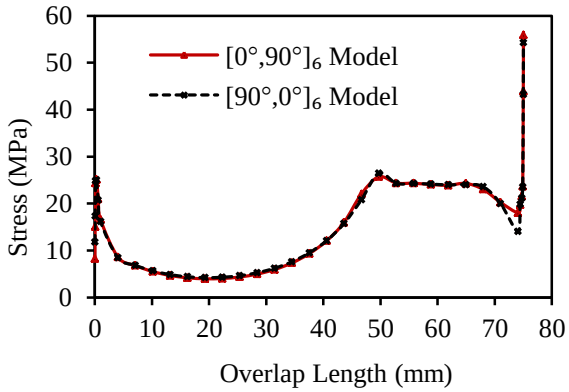

Figure 14. Maximum Principal Stress Distribution along the Upper of Adhesive Layer for various Models with 75 mm Overlap at Failure Loads.

A further data path was created through the thickness of the composite laminate near the centre of the DLS joint in order to show stress distribution through the various layers. See Figure 15. Different DLS joints subjected to failure tensile loading, tensile (S11), peel (S22) and shear (S12) stresses distribution, through the thickness of adhesive and the CFRP laminate with different stacking sequences $[0^o,90^o]_6$ and $[90^o,0^o]_6$models, are given in Figure 16 and Figure 17

respectively. The curves demonstrate the values obtained at the interfaces between each layer of the composite laminate. These curves show that the ply stacking sequences appear to have considerable influence on the stress distribution between layers of the composite laminate.

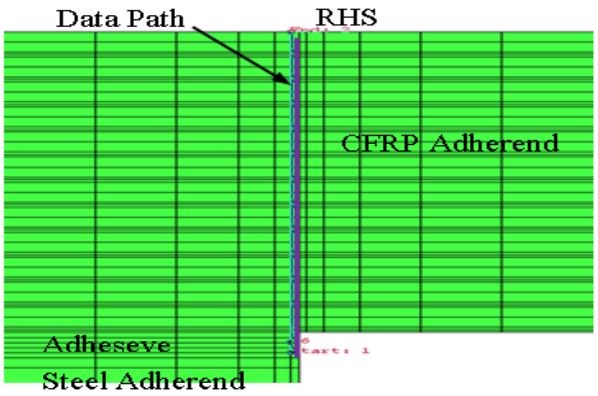

Figure 15. Data path Through the Thickness of the Adhesive and CFRP Laminate (at RHS).

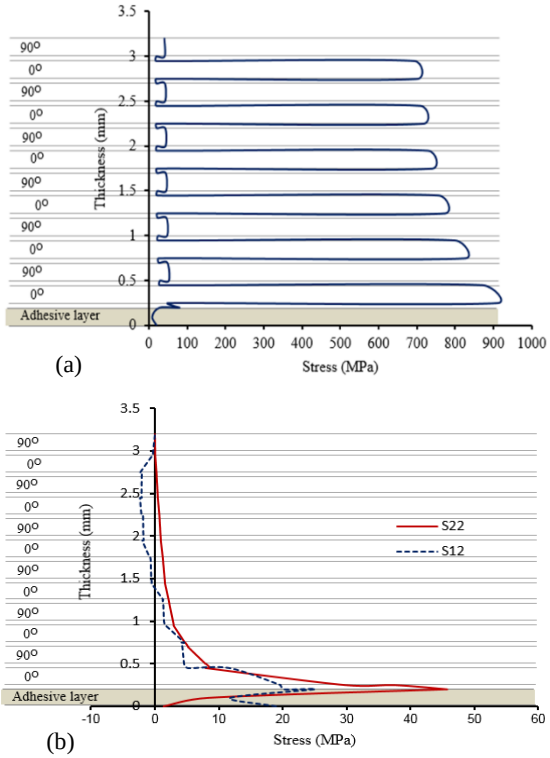

Figure 16 Stress Distributions Through the Thickness of Adhesive and CFRP Laminate of $[0^o,90^o]_6$ Model; (a)Tensile Stress (S11), (b)Peel Stress (S22) and Shear Stress (S12) at Data Path (see Figure 15)

In general, for the two models with different ply stacking sequences, it can be seen that the tensile stress results clearly show a step-wise distribution of stresses, due to discontinuities in material properties between plies. Important results obtained from these curves can be outlined as follows:

- In both models, stress concentration decreases from the first layer to the last one.
- When tensile stress (S11) distributions in load direction are examined, it can be seen that stress concentration is higher at 0^o layers, see Figure 16a and 17a.
- When peel stress (S22) distributions, which are important for the failure of the joint, are examined, it can be detected that in $[0^o,90^o]_6$ model stress is higher at the upper interface of the adhesive layer in (RHS) compared to the lower interface, see Figure 14b. On the other hand, for $[90^o,0^o]_6$ model the stresses are lower than those occurring at the $[0^o,90^o]_6$ model, see Fig. 17b. This directly changes the mode of failure occurring in the joint.
- In the adhesive layer of the $[0^o,90^o]_6$ model, shear stress (S12) value near the centre of the joint (RHS) is higher than that of $[90^o,0^o]_6$ model, see Figure 16b and 17b.

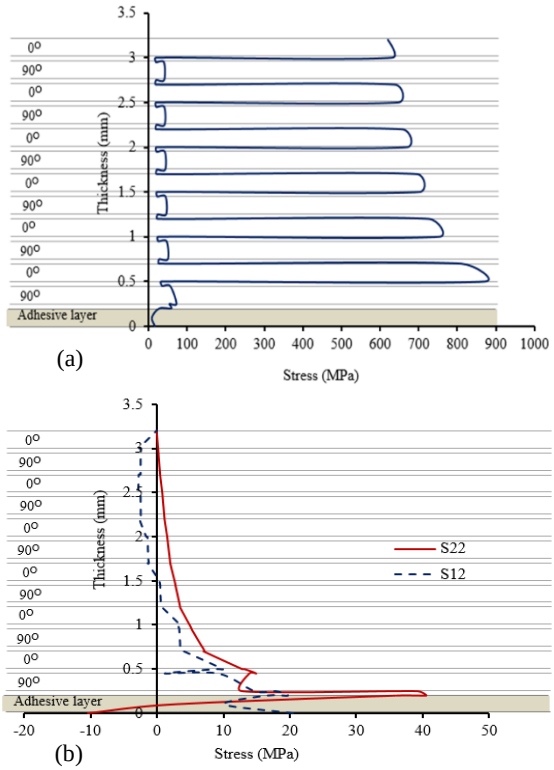

Figure 17 Stress Distributions through the Thickness of Adhesive and CFRP Laminate of $[90^o,0^o]_6$ Model; (a)Tensile Stress (S11) , (b)Peel Stress (S22) and Shear Stress (S12) at Data Path (see Figure15)

V. CONCLUSIONS

It is clear that the use strength-limit modelling in FEA provide good failure predictions within adhesive joints including CFRP delamination. The peak stresses ocurred at the ends of adhesive layer but the largest stress was induced in the right-hand side of the adhesive layer. The reason for this is that the CFRP adherent pulled the adhesive layer upwards. As such a large stress accumulated within the adhesive and caused failure to initiate at the right-hand side of the adhesive. This concurs with the failure witnessed during the

experiments. The critical stresses within the DLS model, a progressive damage analysis was conducted. This analysis concluded that damage initiates at the centre of the joint. The following specifice conclusions might be drawn:

- The modelling approach for including the matrix resin in-between the plies provides a better account for the CFRP delamination, for strength limit approache.
- The adhesive plastic zone length is nearly constant when increasing the overlap length of the DLS joint.
- Increased joint strength is obtained with increased outer adherend (CFRP) thickness.
- Increased upper adherend thickness shows significant reductions in the stress levels occurring at the joint centre (RHS), especially in peel stresses.
- Failure initiation of steel/composite joints occurs very close to the middle of DLS joint at the lower ply of CFRP.
- The fiber orientation and ply stacking sequence had a significant effect on the stress distribution and the failure mode.
- With the 90^o top ply, the failure does not occur at the adhesive bond line but is initiated by a transverse crack next to the $90^o/0^o$ interface leading to delamination failure of the outer adherend.
- The experimental results indicate that if the 0^o ply in the neighbourhood of the adhesive can achieve 5% stronger joint.

ACKNOWLEDGMENT

The author would like to thank the University of Glasgow for supporting the experimental work.

REFERENCES

[1] R.D.S.G. Campilho, M.F.S.F. de Moura, and J.J.M.S. Domingues, "*Modelling single and double lap repairs on composite materials*," *Composites Science and Technology*, vol. 65, p. 1948–1958, 2005.

[2] G.R.Wooley, and D.R Carver, "*Stress concentration factors for bonded lap joint*," *Journal of Aircraft* , vol. 8, p. 817–820, 1971.

[3] J.A. Harris, and R.D. Adams, *"Strength prediction of bonded single lap joints by nonlinear finite element methods*," *International Journal Adhesion and Adhesives*, vol. 4, pp. 65-78, 1984.

[4] N.A. Yahya, and S.A. Hashim, "*Stress analysis of steel/carbon composite double lap shear joints under tensile loading*," *Proc IMechE Part L: Journal of Materials: Design and Applications*, vol. 230, no. 1, p. 88–104, 2016.

[5] L.F.M. da Silva,R.J.C. Carbas,G.W. Critchlow,M.A.V. Figueiredo, and K. Brown, "*Effect of material, geometry, surface treatment and environment on the shear strength of single lap joints*," *International Journal Adhesion and Adhesives*, vol. 29, pp. 621-632, 2009.

[6] S. Feih, and H.R. Shercliff, "*Adhesive and composite failure prediction of single-L joint structures under tensile loading*," *International Journal Adhesion and Adhesives*, vol. 25, pp. 47-59, 2005.

[7] R.A. Odi and C.M. Friend, " *An improved 2D model for bonded composite joints*.," *International Journal of Adhesion and Adhesives*, vol. 24, pp. 389-405, 2004.

[8] M.D. Aydin, A. Özel, and S. Temiz, "*Non-linear stress and failure analyses of adhesively-bonded joints subjected to a bending moment*," *Journal of Adhesion Science and Technology*, vol. 18, p. 1589–1602, 2004.

[9] B.B. Bachir, B. Achour, M. Berrahou, D. Ouinas, and X. Feaugas, "*Numerical estimation of the mass gain between double symmetric and single bonded composite repairs in aircraft structures*," *Material and Design*, vol. 31, p. 3073–3077, 2010.

[10] A.G. Magalhaes, M.F.S.F. de Moura, and J.P.M. Gonçalves, " *Evaluation of stress concentration effects in single-lap bonded joints of laminate composite materials*," *Internatinal Journal of Adhesion and Adheseve*, vol. 25, pp. 313-319, 2005.

[11] S. Akpinar, "*Effects of laminate carbon/epoxy composite patches on the strength of double-strap adhesive joints: Experimental and numerical analysis*," *Materials and Design*, vol. 51, p. 501–512, 2013.

[12] R.D. Adams, J. Comyn, and W.C. Wake, Structural adhesive joints in engineering, Dordrecht: Kluwer Academic Publishing, 1997.

[13] ESA PSS-03-203, Structural Materials Handbook, Issue 1, Vol 1. 1994 [Chapter 21].

[14] R.D. Adams, R.W. Atkins, J.A. Harris, and A.J. Kinloch, "*Stress analysis and failure properties of carbon fiber reinforced plastic steel double lapjoints*," *Journal od Adhesion*, vol. 20, p. 29–53, 1986.

[15] T. Schjelderup, and C.G. Gustafson, "*The wedge test approach to mode 1 interlaminar fracture toughness for CFRP*," in *Proceedings of the 6th European Conference on Composite Materials, September 20–24*, 1993.

[16] V. Pocius, Adhesion and Adhesive Technology, An Introduction Alphonsus, ISBN 1-56990-212-7, 1997.

[17] S.A. Hashim et al., "*Fabrication, testing and analysis of steel/composite DLS adhesive joints*," *Ships and Offshore Structures*, vol. 6, no. 1-2, pp. 115-126, 2011.

[18] "Huntsman Advanced Materials, "www.huntsman.com," 2004".

[19] N.A. Yahya, and S.A. Hashim, "*Delamination of thick adherend steel/CFRP laminate connections*," in *The European Adhesion Conference (9th EURADH)*, Friedrichshafen/Germany, September 2012.

[20] Z. Wu, *"Stress concentration analyses of bi-material bonded joints without inplane stress singularities*," *International Journal of Mechanical Sciences*, vol. 50, pp. 641-648, 2008.

[21] S.A. Hashim, M.J. Cowling, and S. Lafferty, "*The integrity of bonded joints in large composite pipes*," *International Journal of Adhesion and Adhesives*, vol. 18, pp. 421-429, 1998.

BIOGRAPHIES

Najeeb Ali Yahya was born in Surman /Libya, on March 30, 1967. He received B.Sc. degree in Mechanical and Production from University of Sirte/Libya in 1990. He got M.Sc. degree in Solid Mechanics and Vehicle Design from Beihang University/China in 2001. Moreover, he got Ph.D. degree in Mechanical from the Glasgow University/UK in 2015. Currently Assistant Professor in the Department of Mechanical and Industrial Engineering (MIE) at Zawia University/Libya. His research field is in Applied Mechanics and Composite Materials.